GAS HOLDUP AND VOLUMETRIC LIQUID-PHASE MASS TRANSFER COEFFICIENT IN A GEL-PARTICLE SUSPENDED BUBBLE COLUMN WITH DRAUGHT TUBE

KOZO KOIDE, KEIJI SHIBATA, HIROYUKI ITO, SANG YEUL KIM* AND KAZUHISA OHTAGUCHI

Department of Chemical Engineering, Tokyo Institute of Technology, Tokyo 152

Key Words: Mass Transfer, Bubble Column, Gas Holdup, Draught Tube, Solid Particles, Gel, Slurry Reactor

The effects of column dimensions, gas velocity and properties of the liquid and the gel particles on gas holdup ε_G and volumetric liquid-phase mass transfer coefficient k_La in a gel-suspended bubble column with a draught tube and a conical bottom were studied experimentally in a liquid-solid batch operation. The presence of suspended gel particles in the column reduces values of ε_G and k_La, and the degree of reductions due to addition of gel particles to the column increases with increasing gel-particle concentration. Based on these observations, empirical equations of ε_G and k_La applicable to columns of 0.14–0.3 m diameter are proposed.

Introduction

A solid-suspended bubble column with a draught tube and with a conical bottom (usually with a $\pi/3$ rad angle) is often called a pachuca tank and is used widely for leaching ores.[8] Recently, it has drawn attention as a bioreactor. In this case cells, immobilized cells or enzymes, having densities only slightly higher than that of water, and used as suspended particles.

To design a column of this type as a bioreactor, gas holdup ε_G and volumetric liquid-phase mass transfer coefficient k_La should be known. A few research works[3,11] have been reported on ε_G and k_La and in a column with a draught tube and with suspended particles of glass, bronze and activated carbon. Also, a few works[12-15,17] have been done for a column with suspended-solid particles of low density and without a draught tube.

The purpose of this study is to clarify experimentally the effects of column dimensions, gas velocity and the properties of liquid and solid particles on ε_G and k_La in a bubble column with a draught tube and with suspended solids of low-density calcium alginate gel particles in liquid-solid batch operation.

1. Experimental

The experimental apparatus used in this work is shown in **Fig. 1**. The dimensions of plexiglass column used are shown in **Table 1**. The column bottom consists of a conical section with a cone angle of $\pi/3$rad, the details of which are shown elsewhere,[3] and a perforated plate is used as a gas distributor. The perforated plate is covered with a stainless steel wire gauze of 300 mesh to prevent solid particles from penetrating to the gas distributor through the holes, and the holes of the gas distributor are oriented in triangular pitch. Details of the gas distributors are shown in **Table 2**.

The liquids used in this work were demineralized water and aqueous solutions of glycerol, glycol, barium chloride and sodium sulfate. The values for the static slurry height H_L above the gas distributor are shown in Table 1. The operating temperature was kept at 298.2 ± 0.5K. **Table 3** shows physical properties of the liquids.

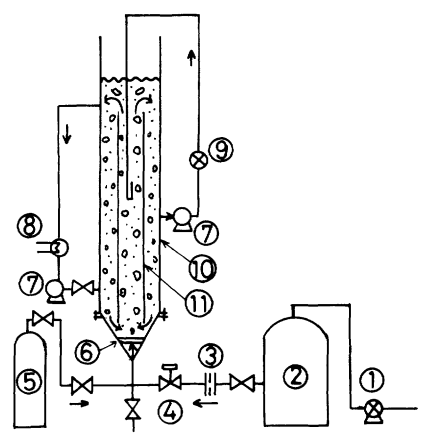

Fig. 1. Experimental apparatus.
1, air compressor; 2, buffer tank; 3, orifice; 4, solenoid valve; 5, nitrogen bomb; 6, gas distributor; 7, pump; 8, heat exchanger; 9, oxygen analyzer; 10, column; 11, draught tube

Received March 5. 1991. Correspondence concerning this article should be addressed to K. Koide. *S. Y. Kim is now with Dept. of Chem. Eng., Dong-A Univ., Pusan 604-714, Korea.

Table 1. Dimensions of apparatus

D_o [m]	D_i* [m]	H [m]	H_L [m]	$L\times10^2$ [m]	Perforated plate**
0.140	0.066	1.40	1.54	3.0	P1
0.140	0.082	0.70	0.84	3.0	P1
0.140	0.082	1.40	1.54	3.0	P1
0.140	0.082	2.10	2.24	3.0	P1
0.140	0.094	1.40	1.54	3.0	P1
0.140	0.104	1.40	1.54	3.0	P1
0.218	0.128	1.40	1.58	4.8	P2
0.300	0.190	1.40	1.68	6.2	P2

* $t_w=3$ mm for $D_i\leqq0.128$ m and 5 mm for $D_i=0.190$ m.
** Dimensions of perforated plate are shown in Table 2.

Table 2. Dimensions of perforated plates

Gas distributor*	D_d [m]	δ [mm]	N [—]
P1	0.035	3	3
P2	0.086	3	10

* The distributor was covered with a stainless steel wire gauze of 300 mesh.

Table 3. Properties of liquids at 298.2K

Liquid*	ρ_L [kg·m^{-3}]	$\mu_L\times10^3$ [Pa·s]	$\sigma_L\times10^3$ [N·m^{-1}]	$D_L\times10^9$ [m^2·s^{-1}]	Crk^2/σ_L [—]
W	997	0.894	72.0	2.42	0
31GL	1075	2.35	69.8	0.975	35.1
66GL	1168	12.5	67.5	0.194	53.9
74EG	1083	5.49	54.4	0.422	38.5
100BC	1013	1.06	72.4	2.06	6.26
270BC	1036	1.16	73.6	1.88	16.6
400SS	1048	1.50	73.7	1.45	25.2

* W: water; 31GL and 66GL: 31.5 and 66.2 wt.% glycerol aq. solns; 74EG: 74.0 wt.% ethylene glycol aq. soln; 100BC and 270BC: 100 and 270 mol·m^{-3} $BaCl_2$ aq. solns; 400SS: 400 mol·m^{-3} Na_2SO_4 aq. soln.

Particles of Ca-alginate gel, used as the solid particles, were made by dropping 1 wt% Na-alginate aq. soln into 2 wt% $CaCl_2$ aqueous solution from a syringe.[10] The sizes of the gel particles were varied by changing the diameter of the needle attached to the syringe. The particles were almost spherical, and the volume-mean diameter d_p was determined from photographs of the particles. The terminal velocity V_t of a single particle in stagnant liquid was calculated on the basis of d_p. Gel particle properties are shown in **Table 4.** The concentration ϕ_S of gel particles was varied in the range of 0—20 vol.%, and air was dispersed into column through a gas distributor at a gas velocity suficient to suspend all the gel particles in the column. During each run, liquid and gel particles were neither fed nor discharged.

The average gas holdup ε_G was calculated by Eq. (1), using the data of H_L and aerated slurry height H_F which were determined by visual observation.

Table 4. Properities of gel particles at 298.3 K

Liquid	$d_p\times10^3$ [m]	$V_t\times10^2$ [m·s^{-1}]	ρ_S [kg·m^{-3}]
W	1.88	1.39	1013
	2.83	2.14	1013
	2.89	2.18	1013
	3.98	2.99	1013
31GL	3.01	0.920	1083
66GL	2.94	0182	1173
74EG	2.70	0.363	1089
100BC	2.55	2.24	1035
270BC	2.56	3.06	1073
400SS	3.19	1.00	1054

$$\varepsilon_G=\frac{(H_F-H_L)}{\left\{H_F-\frac{\sqrt{3}}{2}(D_o-D_d)\right\}+\frac{\sqrt{3}}{6D_o^2}\{D_o^3-D_d^3\}-\frac{V_i}{S_o}} \quad (1)$$

Physical absorption of oxygen from the air by the liquid was employed to determine k_La. Firstly, oxygen in the liquid was purged by dispersing nitrogen gas into the liquid until the oxygen concentration in the liquid fell to about 0.4 ppm. After the nitrogen feed was stopped and the gels settled down, the initial concentration c_0 of dissolved oxygen in the liquid was measured with the dissolved oxygen analyzer (9) shown in Fig. 1, where the liquid in the column was circulated by pump (7) in Fig. 1. Then solenoid valve (4) was opened to disperse air into the column during a certain period, after which the valve was closed and the concentration c of dissolved oxygen was measured. These operations of desorption and absorption of oxygen were carried out three times, changing the period t of supplying air to the column, and then the relation of c vs. t was obtained. For the data taken by this method a linear relationship of $\log(c_i-c)/(c_i-c_0)$ *vs.* t was obtained, where c_i and c_o are respectively the saturated and intial concentration of dissolved oxygen. The slope of this line was used to determine k_La by the method of Sun *et al.*[15] where the effect of intraparticle diffusion of oxygen during gas dispersion was taken into consideration. The diffusivity of oxygen in gel was assumed to be 0.85 times that in liquid.[15,16]

2. Results and Discussion

2.1 Experimental results of ε_G and k_La

Experimental results of ε_G and k_La shown in this work were obtained under the condition that all the particles were suspended in the column.

Figure 2 shows that both ε_G and k_La increase with increasing U_G and decrease with increasing concentration ϕ_S.

Figure 3 shows that the gel-particle diameter d_p has no effect on either ε_G or k_La.

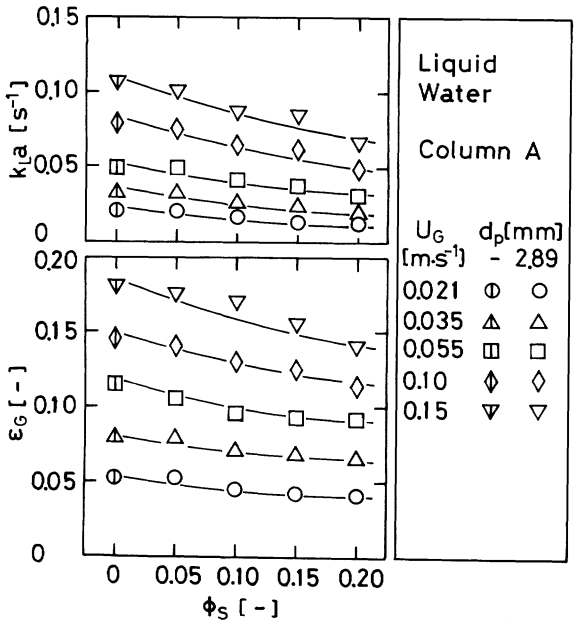

Fig. 2. Effects of gas velocity and solid concentration on ε_G and k_La
Column A: $D_o=0.14$ m, $D_i=0.082$ m, $H=1.40$ m, $H_L=1.54$ m, $L=0.03$ m, $D_d=0.035$ m

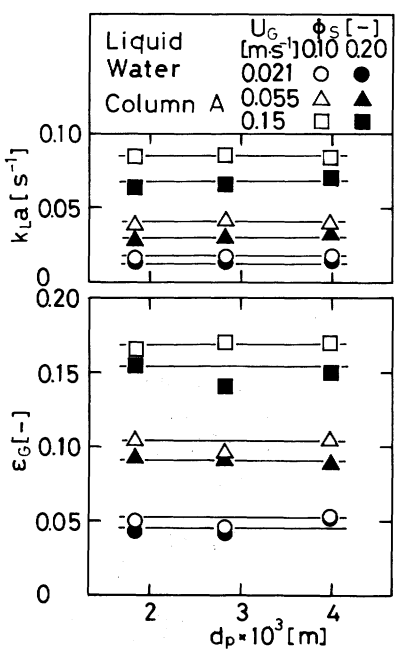

Fig. 3. Effect of gel-particle diameter on ε_G and k_La.

Figure 4 shows that ε_G for $\phi_s=0.2$ is higher in the column having a larger value of D_i/D_o, whereas D_i/D_o has almost no effect on k_La. This might be due to the fact for the same D_o the column having a large value of D_i/D_o has a large cross-sectional area in the draughtt tube where the gas holdup is larger and the specific gas liquid interfacial area smaller than those in the annulus.[5]

Figure 5 shows that the length H of the draught tube has almost no effect on ε_G and k_La.

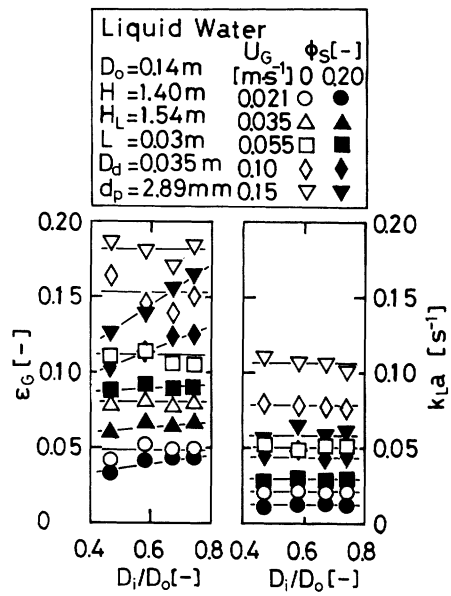

Fig. 4. Effect of draught-tube diameter on ε_G and k_La

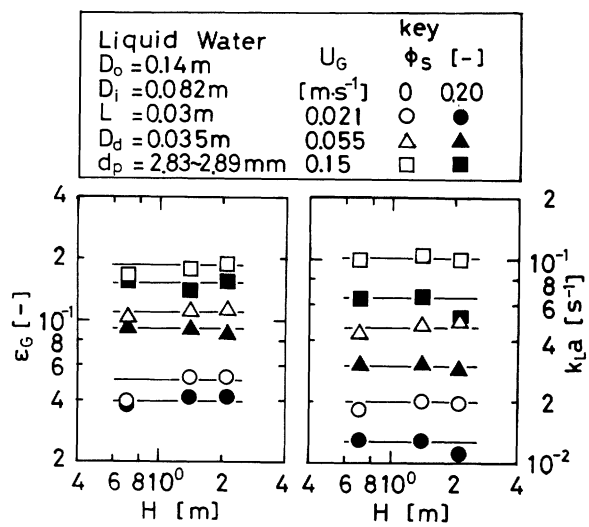

Fig. 5. Effect of draught-tube length on ε_G and k_La

Figure 6 shows that when D_i/D_o is constant the inner diameter D_o of the column has no effect on ε_G, although k_La increases with increasing D_o. The circulating liquid flow in a larger column seems more turbulent near the lower end and the upper end of the draught tube, and this might enhance the gas-liquid mass tranfer in a large column.

Figure 7 shows that the values of ε_G in 31.5 wt.% glycerol aqueous solution are higher than those in water, through the viscosity of the solution is higher than that of water. The reason might be that, because the glycerol aqueous solution has relatively high frothing ability[6,7], bubble coalescence is hindered. However, the values for ε_G in 66.2 wt% glycerol aqueous solution are lower than those in water, since the viscosity of the solution is much higher than that of water, and bubble coalescence occurs more easily

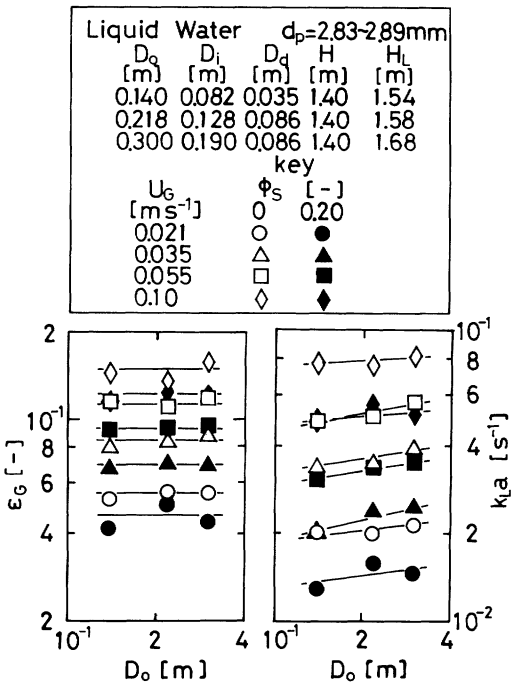

Fig. 6. Effect of column diameter on ε_G and k_La

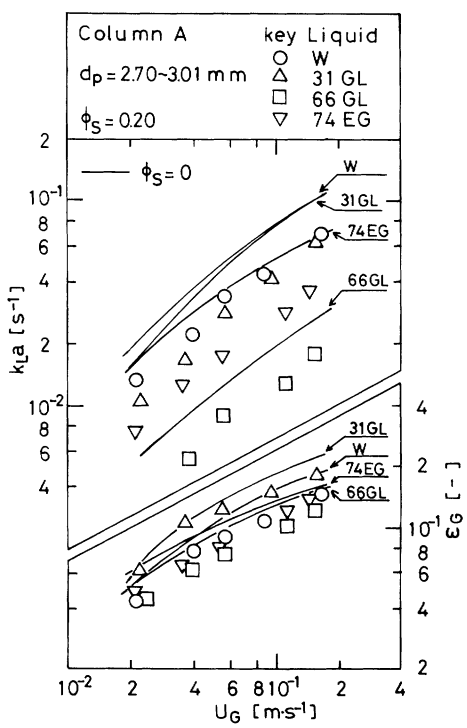

Fig. 7. Effect of liquid properties on ε_G and k_La

in a highly viscous liquid. Figure 7 also shows that the value of k_La decreases with increasing liquid viscosity.

Figure 8 shows that the values of ε_G and k_La in 270 mol/m^3 $BaCl_2$ aqueous solution and Na_2SO_4 aqueous solution higher than those in water. This might be due to the fact that in these solutions bubble coalescence is hindered, i.e. their frothing abilities are

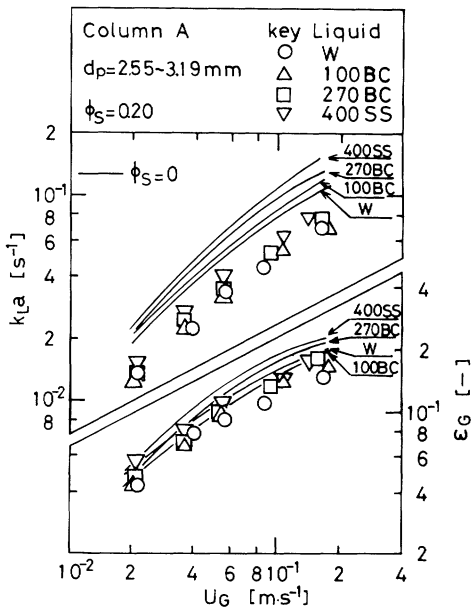

Fig. 8. Effect of inorganic electrolyte on ε_G and k_La

relatively high, and thus bubble sizes are smaller than those in water.[3,6,7]

2.2 Correlation of ε_G and k_La

The effects of U_G, column dimensions and the properties of liquids on ε_G and k_La are similar to those in the previous work,[3] where glass and bronze spheres (ρ_s=2,500—8,700 kg/m^3) were used. However, both ε_G and k_La decrease with increasing terminal velocity V_t of the solid particle[3], whereas the gel-particle diameter d_p has no effect on ε_G and k_La as shown in Fig. 3, which means that V_t has no effect on ε_G and k_La.

Therefore, the same method as that in the previous work[3] was used, to correlate ε_G and k_La with experimental conditions. Firstly, ε_G and k_La in columns without solid particles were correlated with experimental conditions. Secondly, these correlations of ε_G and k_La were modified to include the effect of solid particles on ε_G and k_La.

Types of empirical equations Eqs. (2) and (3) for ε_G and k_La similar to those in the previous paper[3] were used except for the term including the effect of solid particles. Numerical constants in Eqs. (2) and (3) were decided by the direct search method[2] using the data observed in this work, where frothing ability of the liquid was expressed by Marrucci's parameter[9], Crk^2/σ_L,* and the values of Crk^2/σ_L used in this work are shown in Table 2.

* Details of determining this parameter are shown in the previous paper.[7]

$$\frac{\varepsilon_G}{(1-\varepsilon_G)^4}=0.130\left(\frac{U_G\mu_L}{\sigma_L}\right)^{0.890}M_o^{-0.270}\left(\frac{D_i}{D_o}\right)^{0.057}\times\left[1-0.369\left\{1-\exp\left(-0.046\frac{Crk^2}{\sigma_L}\right)\right\}\right]^{-1}\times(1-4.20\phi_S^{1.69})^{-1} \quad (2)$$

The average error in estimating ε_G by Eq. (2) was within 9.4% for 260 data in the experimental ranges of $2.48\times10^{-4}\leqq(U_G\mu_L/\sigma_L)\leqq3.24\times10^{-2}$, $1.69\times10^{-11}\leqq Mo\leqq6.67\times10^{-7}$, $0.471\leqq(D_i/D_o)\leqq0.743$, $0\leqq(Crk^2/\sigma_L)\leqq53.9$ and $0\leqq\phi_s\leqq0.20$. **Figure 9** shows that ε_G values estimated by Eq. (2) agree relatively well with those observed experimentally.

$$\frac{k_La D_o^2}{D_L}=\frac{4.04\,Sc^{0.500}Bo^{0.670}Ga^{0.260}\left(\frac{D_i}{D_o}\right)^{-0.047}\varepsilon_G^{1.34}}{1+2.00\,\phi_S^{1.30}} \quad (3)$$

The average error in estimating k_La by Eq. (3) was within 14% for 260 data in the experimental ranges of $3.71\times10^2\leqq Sc\leqq5.52\times10^4$, $2.66\times10^3\leqq Bo\leqq1.22\times10^4$, $2.35\times10^8\leqq Ga\leqq3.29\times10^{11}$, $0.471\leqq(D_i/D_o)\leqq0.743$, $1.69\times10^{-11}\leqq Mo\leqq6.67\times10^{-7}$, $3.79\times10^{-2}\leqq\varepsilon_G\leqq2.24\times10^{-1}$ and $0\leqq\phi_S\leqq0.20$. **Figure 10** shows that k_La values estimated by Eq. (3) agree relatively well with those observed experimentally.

2.3 Comparison of this work with the previous ones

Koide *et al.*[3] have proposed empirical equations for ε_G and k_La in a 0.1—0.3 mϕ bubble column with a draught tube and with supended solid particles of glass and bronze. **Figure 11** shows that their equation for ε_G does not express well the effect of solid particles on ε_G. This discrepancy might be due to the fact that the equation is based on data of ε_G for slurries of low concentrations ($\phi_s=0$—0.08) and of glass and bronze particles of which the densities ($\rho_s=2500-8770$ kg/m^3) are much higher than those of the gel particles used in this work. Figure 11 shows also that the values of k_La estimated from their empirical equation agree relatively well with those observed in this work.

Muroyama *et al.*[11] have reported that k_La in a column similar to that used in this work is not affected by ϕ_s and increases with increasing gas velocity and column diameter, and have proposed an empirical equation for k_La in the air-water-activated carbon particles ($\rho_s=1300$ kg/m^3) system. The values for k_La estimated from their empirical equation agree relatively well with those for $\phi_s=0$ but not with those for $\phi_s\neq0$.

Conclusion

The presence of suspended gel particles in a bubble column with a draught tube and with a conical bottom reduces values of the gas holdup ε_G and the volumetric

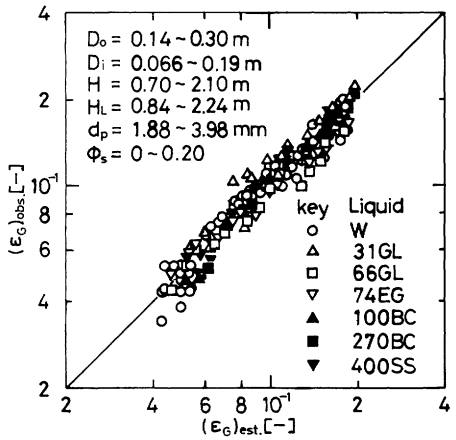

Fig. 9. Comparison of ε_G values estimated by Eq. (2) with those observed in this work

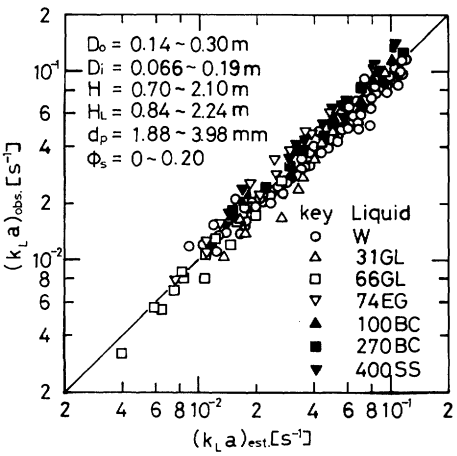

Fig. 10. Comparison of k_La values estimated by Eq. (3) with those observed in this work

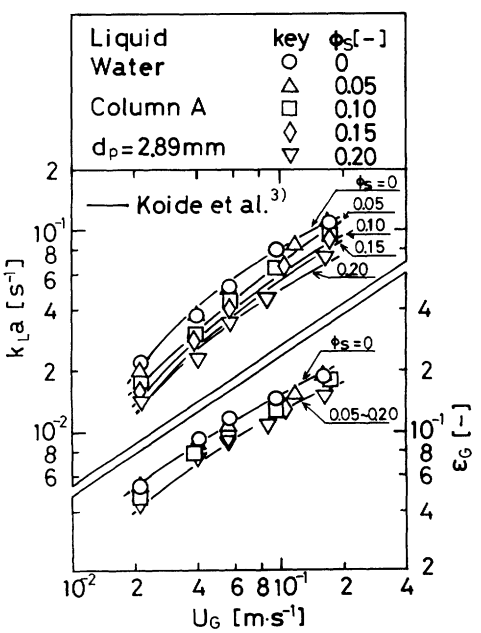

Fig. 11. Comparison of ε_G and k_La values estimated by the equations of Koide *et al.*[3] with those observed in this work

liquid-phase mass transfer coefficient k_La. The reductions of ε_G and k_La values due to addition of gel particles to the column increase with increasing gel-particle concentration, but is not affected by the gel-particle diameter d_p in the range of $d_p=1.88$–3.98 mm. Based on these observations, empirical equations of ε_G and k_La are proposed.

Nomenclature

A	=	Hamaker constant	[J]
a	=	specific gas-liquid interfacial area based on aerated liquid volume	[m^{-1}]
Bo	=	$\rho_L D_0^2 g/\sigma_L$, Bond number	[—]
C	=	$\frac{2c_1}{vRT}\left(\frac{d\sigma_L}{dc_1}\right)^2 \frac{1}{\{1+(d\ln f_1/d\ln c_1)\}\{1+(x_1v_1/x_2v_2)\}}$	[N]
Crk^2/σ_L	=	parameter of bubble coalescence proposed by Marrucci[9]	[—]
c	=	concentration of dissolved oxygen	[$mol\cdot m^{-3}$]
c_i	=	saturated concentration of dissolved oxygen	[$mol\cdot m^{-3}$]
c_0	=	initial concentration of dissolved oxygen	[$mol\cdot m^{-3}$]
c_1, c_2	=	concentration of components 1 and 2 in liquid	[$mol\cdot m^{-3}$]
D_d	=	diameter of gas distributor	[m]
D_i	=	inner diameter of draught tube	[m]
D_L	=	diffusivity of dissolved oxygen	[$m^2\cdot s^{-1}$]
D_O	=	column diameter	[m]
d_p	=	average diameter of gel particles	[m]
f_1	=	activity coefficient of component 1 in liquid	[—]
Ga	=	$gD_o^3\rho_L^2/\mu_L^2$, Galilei number	[—]
g	=	gravitational acceleration	[$m\cdot s^{-2}$]
H	=	length of draught tube	[m]
H_F	=	level of aerated slurry during operation	[m]
H_L	=	static slurry height above gas distributor	[m]
k	=	$(12\pi\sigma_L/Ar)^{1/3}$	[m^{-1}]
k_L	=	liquid-phase mass transfer coefficient	[$m\cdot s^{-1}$]
k_La	=	volumetric liquid-phase mass transfer coefficient based on aerated slurry volume	[s^{-1}]
L	=	vertical clearance between lower end of draught tube and wall of conical bottom	[m]
M_o	=	$g\mu_L^4/\rho_L\sigma_L^3$, Morton number	[—]
N	=	number of holes in gas distributor	[—]
P	=	pitch of holes in gas distributor	[—]
R	=	gas constant	[$J\cdot K^{-1}\cdot mol^{-1}$]
r	=	radius of bubble	[m]
Sc	=	$\mu_L/D_L\rho_L$, Schmidt number	[—]
S_o	=	cross-sectional area of column	[m^2]
T	=	liquid temperature	[K]
t	=	time	[s]
t_w	=	wall thickness of draught tube	[m]
U_G	=	gas velocity based on cross section of column and based on average static pressure in column	[$m\cdot s^{-1}$]
V_i	=	volume of draught tube	[m^3]
V_t	=	terminal velocity of a single particle in stagnant liquid	[$m\cdot s^{-1}$]
v_1, v_2	=	molar volume of components 1 and 2 in liquid	[$m^3\cdot mol^{-1}$]
x_1, x_2	=	mole fraction of components 1 and 2 in liquid	[—]
δ	=	hole diameter in gas distributor	[m]
ε_G	=	gas holdup	[—]
ε_L	=	liquid holdup	[—]
ε_S	=	solid holdup	[—]
μ_L	=	liquid viscosity	[Pa·s]
ν	=	total number of moles of ions per mole of electrolyte or 1 for non-electrolyte	[—]
ρ_L	=	liquid density	[$kg\cdot m^{-3}$]
ρ_s	=	solid density	[$kg\cdot m^{-3}$]
σ_L	=	liquid surface tension	[$N\cdot m^{-1}$]
ϕ_s	=	$\varepsilon_S/(\varepsilon_S+\varepsilon_L)$, solid concentration in slurry	[—]

〈Subscripts〉

est.	=	estimated value
obs.	=	observed value

Literature Cited

1) Akita, K. and F. Yoshida: *Ind. Eng. Chem., Process Des. Develop.*, **12**, 76 (1973).
2) Himmelblau, D. M.: "Process Analysis by Statistical Methods", p. 178, John Wiley & Sons (1970).
3) Koide, K., K. Horibe, H. Kawabata and S. Ito: *J. Chem. Eng. Japan*, **18**, 248 (1985).
4) Koide, K., K. Horibe, H. Kawabata and S. Ito: *J. Chem. Eng. Japan*, **17**, 368 (1984).
5) Koide, K., K. Horibe, H. Kitaguchi and N. Suzuki: *J. Chem. Eng. Japan*, **17**, 547 (1984).
6) Koide, K., K. Kurematsu, S. Iwamoto, Y. Iwata and K. Horibe: *J. Chem. Eng. Japan*, **16**, 413 (1983).
7) Koide, K., H. Sato and S. Iwamoto: *J. Chem. Eng. Japan*, **16**, 407 (1983).
8) Lamont, A. G. W.: *Can. J. Chem. Eng.*, **31**, 153 (1958).
9) Marrucci, G.: *Chem. Eng. Sci.*, **24**, 975 (1969).
10) Mikami, Y.: *Saibō Kōgaku*, **5**, 959 (1986).
11) Muroyama, K., A. Yasunishi and Y. Mitani: Proceedings of the Third Pacific Chem. Eng. Congress, **1**, 303 (1983).
12) Sauer, T. and D.-H. Hempel: *Chem. Eng. Technol.*, **10**, 180 (1987).
13) Sun, Y., T. Nozawa and S. Furusaki: *J. Chem. Eng. Japan*, **21**, 15 (1988).
14) Sun, Y. and S. Furusaki: *J. Chem. Eng. Japan*, **21**, 20 (1988).
15) Sun, Y. and S. Furusaki: *J. Chem. Eng. Japan*, **22**, 556 (1989).
16) Sun, Y., S. Furusaki, A. Yamauchi and K. Ichimura: *Biotechnol. Bioeng.*, **34**, 55 (1989).
17) Tang, W.-T. and L.-S. Fan: *Ind. Eng. Chem. Res.*, **29**, 128 (1990).

(Presented in part at the 23rd Autumn Meeting of Society of Chemical Engineers, Japan, Kanazawa, October 11, 1990)